Overexpression of the X-Linked Inhibitor of Apoptosis Protects Against Retinal Degeneration in a Feline Model of Retinal Detachment

Sarah J. Wassmer,[1,†] Brian C. Leonard,[2–4] Stuart G. Coupland,[1–4] Adam N. Baker,[3] John Hamilton,[4] William W. Hauswirth,[5] and Catherine Tsilfidis[1–4,*]

Departments of [1]Cellular and Molecular Medicine and [2]Ophthalmology, University of Ottawa, Ottawa, Canada; [3]Ottawa Hospital Research Institute, Regenerative Medicine, Ottawa, Canada; [4]Ottawa Hospital, Eye Institute, Ottawa, Canada; [5]Department of Ophthalmology, University of Florida College of Medicine, Gainesville, Florida. [†]Current address: Schepens Eye Research Institute, Boston, Massachusetts.

Retinal detachment is an acute disorder in humans that is caused by trauma or disease, and it can often lead to permanent visual deficits that result from the death of photoreceptors in the retina. The final pathway for photoreceptor cell death is apoptosis and necroptosis. The X-linked inhibitor of apoptosis (XIAP) has been shown to block both of these cell death pathways. This study tested the effects of XIAP on photoreceptor survival in a feline model of retinal detachment. The study was performed in 12 cats, divided into two experimental groups. Six animals received a subretinal injection of adeno-associated virus (AAV) carrying *XIAP*, and six animals received AAV carrying green fluorescent protein (*GFP*) as a control. Three weeks after viral delivery, retinas were detached by injecting C_3F_8 gas into the subretinal space. Optical coherence tomography revealed that the retinal detachments resolved within 3–6 weeks as the gas was slowly resorbed. Analysis of histological sections through the plane of the detachment showed significant preservation of the photoreceptor layer in AAV-XIAP-treated animals compared to AAV-GFP-treated animals at 9 weeks after the detachment. XIAP-treated detached retinas were similar to intact controls. These studies support the potential for XIAP therapy in the treatment of human retinal detachment.

Keywords: XIAP, apoptosis, retinal detachment, gene therapy, adeno-associated virus

INTRODUCTION

Retinal detachment (RD) occurs when trauma to the eye, accumulation of fluid in the subretinal space, or tractional pulling of the retina by vitreous bands induces a separation between the retinal pigment epithelium (RPE) and the sensory neural retina. The outermost layer of the retina, where the rod and cone photoreceptors reside, depends on the underlying RPE and choroidal vasculature for trophic support and maintenance of homeostasis.[1] Consequently, RD can lead to relatively rapid degenerative changes in the outer retina, with one study suggesting that there are histologic signs of retinal degeneration as early as 1 h after RD in a cat model.[2] Despite the fact that retinal reattachment surgery is anatomically effective, visual acuity is often compromised and depends on the nature and duration of the detachment. Loss of vision is accentuated if the macula—the central area of the retina that provides detailed visual acuity—is involved in the detachment.[2]

Based on animal studies, the final pathway for photoreceptor cell death in RD involves both apoptosis and necroptosis.[3,4] The physical separation of the retina from the underlying RPE leads to an increase in transcription of tumor necrosis factor alpha (*TNF-α*) and activates caspase-8 and caspase-9, ultimately leading to cell death by apoptosis.[5,6] However, apoptosis is only one contributor to cell death in RD. Necroptosis, mediated by the formation of a ripoptosome by receptor interacting proteins (RIP) 1 and 3, is also involved in RD-induced photoreceptor cell death.[7] It has been postulated that inhibition of apoptosis promotes a shift toward necroptosis and that caspase inhibitors alone cannot prevent photoreceptor cell death following RD.[7]

The X-linked inhibitor of apoptosis (XIAP) has the ability to inhibit both apoptosis and necroptosis.[8–10]

*Correspondence: Prof. Catherine Tsilfidis, Ottawa Hospital Research Institute, 501 Smyth Road, Box 511, Ottawa, Ontario, K1H 8L6, Canada. E-mail: ctsilfidis@ohri.ca

DOI: 10.1089/hum.2016.161

XIAP is a direct inhibitor of caspases 3, 7, and 9, and has been previously shown to preserve retinal cells in multiple forms of retinal degeneration.[11–15] Additionally, XIAP has also been shown to control TNF and RIP3-dependent inflammasome formation.[16,17] Furthermore, it has been suggested that XIAP and other members of the inhibitor of apoptosis family (cIAP1 and cIAP2) function as inhibitors of the ripoptosome by direct ubiquitination of its components.[18]

In light of XIAP's roles in caspase-dependent apoptosis, in inflammation and in caspase-independent necroptosis, it was hypothesized that XIAP would protect photoreceptor structure and function following RD. Consistent with this hypothesis, previous work has shown that XIAP can protect photoreceptor structure in a rat model of RD.[15] However, the technical challenges of surgery in the small rat eye prevented both reattachment of the retina and functional testing using electroretinography. As a result, a cat model of RD was developed,[19] and this model was employed to study XIAP efficacy in protecting photoreceptors through detachment and reattachment of the retina. The current study shows that XIAP inhibits TNF-α-induced cell death in photoreceptor cells *in vitro,* and protects outer nuclear layer (ONL) thickness *in vivo*. Histology, optical coherence tomography (OCT) and electroretinography are used to assess XIAP effects on photoreceptor structure and function.

MATERIALS AND METHODS

Animals

Twelve male cats aged ≥8 months were purchased from Liberty Research (Waverly, NY). Animals were housed together in large multilevel enclosures that provided an enriched environment and allowed free movement. Animal procedures were conducted in accordance with the University of Ottawa Animal Care Committee rules and regulations and adhered to the ARVO statement for the Use of Animals in Ophthalmic and Vision Research.

Anesthesia

Felines were given Propofol (1 mL/min; Fresenius Kabi, Richmond Hill, Canada) intravenously or 5% isoflurane (Fresenius Kabi) by aerosol mask before surgery and during the administration of the anesthetic. Animals were administered 0.015 mg/kg of medetomidine (Modern Veterinary Therapeutics, Miami, FL) and 0.1 mg/kg of hydromorphone (Sandoz Canada, Boucherville, Canada) by intramuscular injection and were kept under 2–3% isoflurane throughout all surgical procedures. Normosol fluids (Hospira Healthcare Corp., Saint Laurent, Canada) were provided by intravenous infusion. The antiemetic medication, Cerenia (Zoetis Canada, Kirkland, Canada), was used at a dosage of 0.5 mg/kg in susceptible animals, only when electroretinography was not being performed, as previous studies showed that Cerenia interferes with the electroretinogram (ERG).[19] Vital signs were monitored throughout the procedure, and an intramuscular injection of 0.02 mg of glycopyrrolate (2 mg/mL; Sandoz Canada) was administered if the heart rate significantly decreased during or after surgery. Five minutes before the end of the surgery, the medetomidine was reversed using 0.05–0.06 mg/kg of atipamezole hydrochloride (Modern Veterinary Therapeutics; 5 mg/mL). After surgery, animals received 0.02 mg/kg of buprenorphine (0.3 mg/mL; Sovegal UK Ltd., York, United Kingdom) subcutaneously for pain management.

Virus vector production

A cDNA construct encoding the full-length, open-reading frame of human *XIAP* was cloned into the pTR adeno-associated virus (AAV) vector. The construct had an N-terminal hemagglutinin (HA) tag and was under the control of the human rhodopsin kinase (RK) promoter. Transgene expression was enhanced by a woodchuck hepatitis virus posttranscriptional regulatory element in the 3′ untranslated region of the construct. A RK-GFP construct was similarly generated for use as a control. Serotype 5 recombinant AAV vector was generated and purified as previously described.[20,21]

Surgeries

One drop each of Mydriacyl (1%), Mydfrin (2.5%), and Alcaine (0.5%; Alcon Canada, Mississauga, Canada) were administered to the surgical eye. A three-port pars plana phacofragmentation lensectomy followed by a vitrectomy were performed, as previously described.[19] These procedures gave unobstructed access to the central retina for the delivery of the AAV vector and the induction of the RD. The left eye of six felines received serotype 5 AAV carrying HA-tagged XIAP driven by the RK promoter (AAV-XIAP). The virus was injected into the subretinal space of the superior retina, in close proximity to the optic nerve. A total volume of 100 μL was injected, containing 1×10^{10} vector genomes (vg). Another six animals received 1×10^{10} vg of AAV5.RK.GFP as a control. The posterior chamber was filled with sterile balanced saline salt after the vector injection to maintain intraocular pressure.

Three weeks after vector delivery, a RD was created by administering 8% C_3F_8 gas as close as possible to the viral injection site. A 15–20% RD was created.

After each surgery, the eyes were treated with 5–10 drops of 1.0% w/v atropine sulfate (Chauvin Pharmaceuticals, Surrey, United Kingdom) and covered with Tobradex Ophthalmic Ointment (tobramycin 0.3%, dexamethasone 0.1%; Alcon Canada). The animals were treated four times daily with Tobradex for 10 days post surgery.

Enucleation

Nine or ten weeks post detachment, the left eyes of the animals were surgically removed. In addition to the anesthesia regime described above, 10 mL of 2% xylocaine was injected into the orbit. Buprenorphine and the nonsteroidal anti-inflammatory drug Metacam (0.1 mg/kg of meloxicam; Boehringer Ingelheim, Burlington, Canada) were administered every day for a minimum of 3 days post enucleation. Oral administration of the antibiotic Clavamox (1 mL containing 50 mg of amoxicillin and 12.5 g clavulanic acid; Zoetis) was given to the cats twice daily post enucleation, and oral gabapentin (10 mg/kg) was given for pain relief, as needed. Following complete recovery, animals were adopted out.

OCT and electroretinography

OCT was performed as previously reported.[19] Eyes were imaged before injection of the vector and subsequently every 3 weeks post detachment. After lens removal, a 10+ diopter lens was placed in front of the eye to gain access into the focusing range of the OCT machine. Photoreceptor function was assessed with an Espion e^2 (Diagnosys Systems, Inc., Westford, MA) full-field flash ERG (3 $cd \cdot s/m^2$ on a 30 cd/m^2 background luminance) presented at a rate of 1 Hz. An ERG-Jet (LKC Technologies, Inc., Gaithersburg, MD) was placed on the corneal surface with appropriate corneal hydration. ERGs were recorded with bandpass filtering of 0.3–300 Hz, and 50 sweeps were signal averaged.

Area measurements

Images were taken of hematoxylin and eosin (H&E) sections using the 20× objective on the Zeiss Axio Imager M2 (Carl Zeiss Canada Ltd., North York, Canada) through the plane of the optic nerve. Images were stitched together to obtain a collage of the full retina, and the final image was imported into ImageJ. The ONL was traced in the superior retina (where the detachment was located) from the optic nerve peripherally for a distance of 8,800 μm. The area encompassing the ONL was calculated. In the same region, the area of the whole retina was also measured. The ratio of the ONL area to the whole retinal area was calculated and compared between XIAP- and GFP-treated animals. A similar analysis was conducted in the inferior, intact retina to enable a comparison between detached and control retinas for both GFP- and XIAP-treated eyes. All area measurements were conducted by a researcher (C.T.) who was masked to the experimental status of each of the eyes.

Cell death assays

The transformed cone photoreceptor cell line, 661W, was kindly provided by Dr. M. Al-Ubaiddi.[22] The 661W cells were transfected with pCI-neo containing the full-length coding sequence of human *XIAP*, which was generated from pCM-SPORT6-XIAP (Origene, Rockville, MD), digested with Sal1 and NOT1 to isolate the XIAP coding sequence, and ligated into the pCI-neo vector (Promega, Madison, WI). Transfections were conducted using ExpressIn or Lipofectamine 2000 (Thermo Fisher Scientific, Waltham, MA), according to the manufacturer's instructions. Control cell lines were transfected in a similar manner with the pCI-neo empty vector (EV). Stably expressing cells lines were grown under G418 selection. Three independent cell lines overexpressing XIAP were generated. The line with the best protection in the death assay was used for the results described in the body of the paper. Results obtained with the other two lines can be found in the Supplementary Data (Supplementary Data are available online at www.liebertpub.com/hum). All cell lines were used below passage 15, and XIAP expression was monitored in each assay by Western blot or reverse transcription quantitative polymerase chain reaction.

For the death assays, cells were plated onto six- or 96-well plates at 60% confluency and incubated with mouse recombinant TNF-α at 5 ng/mL (Roche Canada, Mississauga, ON) for 4 days, 1 mM of hydrogen peroxide (Sigma–Aldrich, Oakville, Canada) for 32 h or 15 μM of menadione (Sigma–Aldrich) for 4 h. Cell viability was measured using trypan blue (Sigma–Aldrich) or alamarBlue ® cell viability reagent (Invitrogen, Carlsbad, CA) for six- and 96-well formats, respectively.

Western blot

Retinal protein (20 μg) was electrophoresed on 12% polyacrylamide gels, and transferred onto polyvinylidene membranes. Membranes were blocked for 1 h at 4°C in 5% powdered milk, and incubated overnight at 4°C with antibodies to GST-XIAP (1:5,000 in blocking buffer; courtesy of Dr. Robert Korneluk, University of Ottawa, Canada), Bcl2 (Cell Signaling, Danvers, MA; 1:1,000) or Caspase-3 (Cell Signaling; 1:1,000).

Membranes were washed and incubated for 1 h at room temperature in anti-rabbit horseradish peroxidase or anti-rabbit IRDye 800 (Li-Cor, Lincoln, NE). Proteins were visualized using Pierce Chemiluminescence substrates (Thermo Fisher Scientific) and film, or the Licor imaging system. Multiple exposures were taken of the blots, and densitometry was conducted on blots whose bands were not overexposed to ensure quantification of bands in the linear range of detection.

Immunohistochemistry

Prior to enucleation, a 3-0 Vicryl suture (Ethicon, Somerville, NJ) was used to mark the superior pole of the eye. Enucleated eyes were placed in modified Davidson's fixative and sent to Excalibur Pathology, Inc. (Norman, OK) where they were embedded in wax and sectioned at 6 μm. A subset of the slides were stained by Excalibur Pathology, Inc., with H&E.

For immunohistochemical detection of HA-tagged XIAP, sections were dewaxed and then placed in citrate buffer (10 mM of sodium citrate in water; pH 6) within the Biocare Medical Digital Decloaking Chamber (Biocare, Concord, CA). Slides were removed from the chamber, allowed to cool to room temperature, washed with phosphate-buffered saline (PBS), permeabilized in 0.1% triton in PBS (wash buffer), blocked for 2 h (10% normal goat serum in wash buffer), and incubated for 2 days at 4°C with HA primary antibody (1:100; Roche Canada) diluted in blocking solution. Slides were then washed in wash buffer and incubated with Cy3 secondary antibody (1:500; Jackson ImmunoResearch, West Grove, PA) diluted in PBS. After precisely 2 h, the sections were washed with wash buffer and then PBS, and were mounted in Prolong Gold antifade reagent (Life Technologies; Thermo Fisher Scientific). For specific details for immunofluorescence staining, see Nayagam *et al*.[23]

To detect the GFP signal, autofluorescence in the retinal sections necessitated the use of a colorimetric assay (the ImmPRESS Detection System; Vector Laboratories, Burlingame, CA). All manufacturer procedures were followed, with the exception that no counterstain was used. All sections were imaged using a Zeiss Axio Imager M2 (Carl Zeiss Canada Ltd.).

RESULTS

XIAP protects 661W cone photoreceptor cells in an *in vitro* model of retinal cell death

TNF-α has been shown to mediate photoreceptor cell death in a rodent model of RD.[6] Therefore, the ability of XIAP to protect 661W cone photoreceptor cells from TNF-α-induced cell death was examined. 661W cells were transfected with either plasmid pCI.CMV.XIAP or pCI EV (XIAP and EV, respectively). Three stable XIAP overexpressing cell lines were generated (XIAP1-3; Supplementary Fig. S1), and their ability to protect against TNF-α was assessed. All three lines showed increased protection of 661W photoreceptors cells against TNF-α-induced cell death, accompanied by increased levels of the anti-apoptotic protein Bcl2, and decreased levels of cleaved caspase 3 (see Supplementary Fig. S1). The cell line that was consistently the most robust in neuroprotection assays (XIAP1 in Supplementary Fig. S1) was further characterized and used for the assays described below.

XIAP- and EV-transfected cells were treated with 5 ng/mL of TNF-α in complete medium for 4 days. The mean cell viability from seven independent cell death assays was 60.5% for XIAP and 8.5% for EV cells (significant at $p \leq 0.001$; Fig. 1B, day 4) using the trypan blue exclusion assay. The protective effects of XIAP against TNF-α were further confirmed using the alamarBlue viability assay (Fig. 1C). Since RD has been shown to be associated with oxidative stress in both animal models and human retinal samples,[24–26] the ability of XIAP to protect against menadione and hydrogen peroxide, two potent oxidative stressors, was also tested. In both assays, XIAP overexpression significantly protected the 661W photoreceptor cells (Fig. 1D and E).

XIAP gene therapy in a cat model of RD

In order to test the effects of XIAP overexpression in an *in vivo* model of RD, six domestic felines were subretinally injected with AAV expressing hemagglutinin-tagged XIAP driven by the RK promoter (AAV-XIAP). Another six animals received AAV-GFP as a control. The shallow detachments induced by these injections normally resolve within 24 h and do not create any complications with retinal structure (confirmed by OCT analysis) or function. Three weeks after the viral injection, a RD was induced at the site of the viral delivery (or as close as possible to it) by injecting 8% C_3F_8 gas into the subretinal space. A detachment, spanning approximately 15–20% of the retina, was induced (Fig. 2). C_3F_8 gas was used for the detachments because it is slowly resorbed, allowing a gradual reattachment of the retina over the ensuing weeks without requiring surgical intervention. All detachments were placed in the superior pole of the retina. Animals were examined weekly using

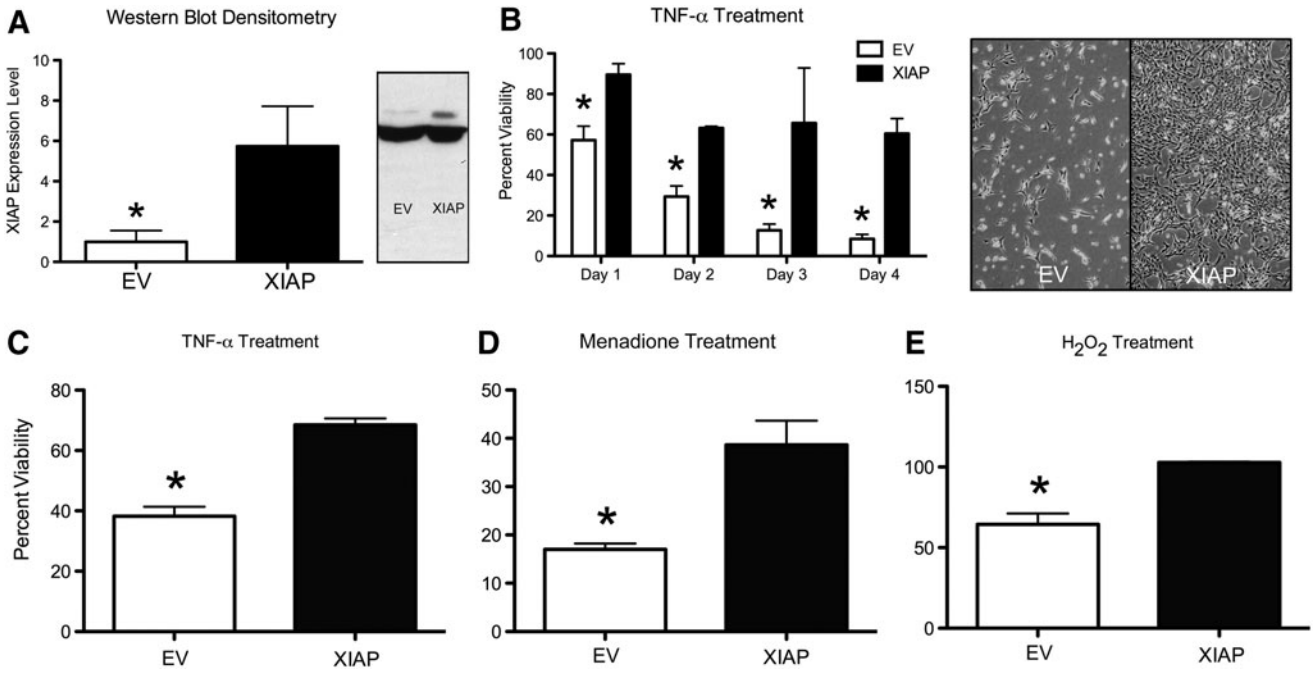

Figure 1. X-linked inhibitor of apoptosis (XIAP) protects 661W photoreceptor cells against various cell death triggers. (**A**) Densitometry analysis of three independent Western blots showing XIAP overexpression in the XIAP1 stably transfected 661W cell line (see Supplementary Fig. S1; $*p \leq 0.02$). XIAP expression (upper band of Western blot) was normalized to the β-actin loading control (lower band) and is shown relative to empty vector (EV) levels. One of the Western blots, probed with GST-XIAP, is shown in the *right* panel. The blot was overexposed to show the endogenous level of XIAP in the EV control. (**B**) XIAP protects 661W cells from 5 ng/mL of tumor necrosis factor alpha (TNF-α) over a 4-day incubation period. Bar graph shows cell survival in comparison to the EV control, assessed using the trypan blue exclusion assay ($*p \leq 0.02$ for day 1, $p \leq 0.01$ for days 2 and 3, and $p \leq 0.0005$ for day 4). Representative images of 661W cells treated with 5 ng/mL of TNF-α for 4 days are shown in the *right* panel. (**C–E**) Cell viability assessed using the alamarBlue assay for 661W cells treated with 5 ng/mL TNF-α for 4 days (**C**) ($*p < 0.002$), 15 μM of menadione for 4 h (**D**) ($*p < 0.02$), and 1 mM of hydrogen peroxide for 32 h (**E**) ($*p < 0.005$). All error bars represent standard error of the mean (SEM). Statistical analysis in (**A**) was conducted using the Mann–Whitney–Wilcoxon test. All other statistical analyses were conducted using Student's *t*-test.

an ophthalmoscope, and retinal function was assessed every 3 weeks with a full-flash ERG. OCT and fundus images were also taken every 3 weeks, concurrent with the ERGs.

Three animals (one XIAP-treated and two GFP-treated) were eliminated from the study because their experimental partial detachments progressed into complete RDs. Despite the precise placement of the viral vectors and the RD, for humane reasons the activity of the animals was not restricted, and the animals' head movement allowed the displacement of the gas bubble throughout the retina in those three animals, resulting in a complete RD.

The two retinotomy sites created by the viral injection and the detachment were visible throughout the experiment (Fig. 3), allowing the same retinal areas to be serially imaged accurately by OCT by reference to these injection sites. These sites were also used to localize the site of the detachments for subsequent histological analysis. The OCT images confirmed that the C_3F_8 gas had been resorbed and the retina had reattached within 3–6 weeks after the detachment (Fig. 4). Specifically, the detachment only presented as small ripples in the retina at 3 weeks, which were almost completely flat and reattached by 6 weeks in most of the animals (see Fig. 4 and Supplementary Fig. S2). However, three animals presented with some complications from the surgeries. XIAP1 showed retinal puckering on the OCT, indicating that the RD had not properly resolved (see Supplementary Fig. S3). XIAP 5 (see Supplementary Fig. S3) had a vitreal hemorrhage, making fundus imaging and OCT impossible at the latest time point. Finally, GFP1 appeared to have both a possible solid detachment (caused by subretinal fluid and folding of the retina), which prevented the acquisition of a clear fundus image, and two additional retinal irregularities aside from the retinotomies associated with viral or gas injections (see Fig. 3 and Supplementary Fig. S4). All of these animals are discussed in more detail below in the context of the histological analysis of the retinas.

XIAP overexpression protects photoreceptor structure in RD

For histological analysis, sagittal sections were taken through the eye in the plane of the optic nerve and 0.3 cm nasal to the plane of the optic

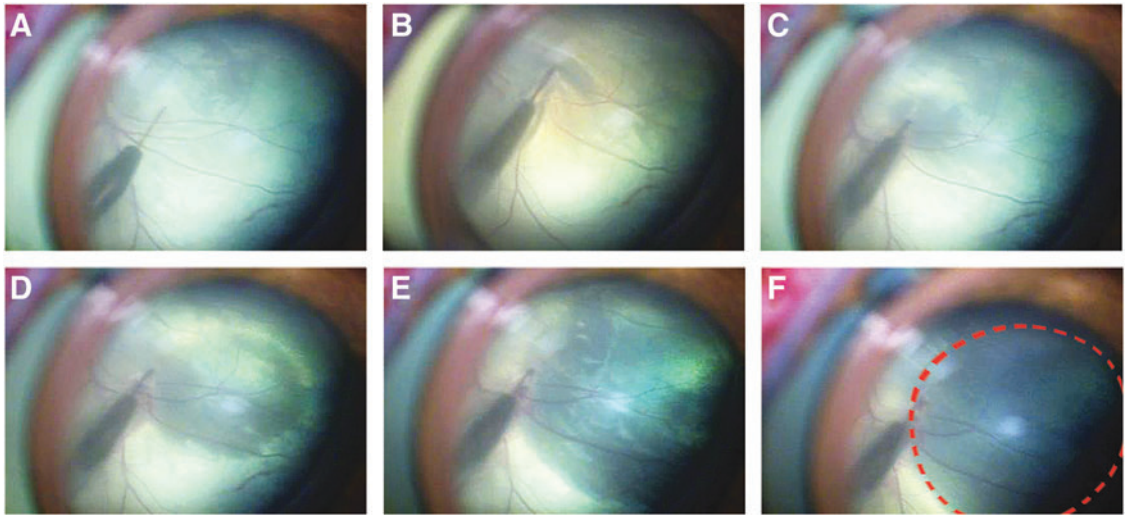

Figure 2. Retinal detachment induced by injection of 8% C_3F_8 gas into the sub-retinal space. An angled 42G subretinal cannula was connected to a syringe containing the C_3F_8 gas via flexible sterile tubing. The gas was slowly injected into the subretinal space until approximately 20% of the retina was detached. (**A–F**) Sequential images showing the growing retinal detachment as C_3F_8 gas in injected. The detachment is outlined in (**F**).

nerve. One or the other of these sections would encompass the sites of the injection and detachment based on the retinotomies visible by OCT. Since the retinas had already reattached at the time that the eyes were sampled, the exact site of the detachment was difficult to ascertain. However, signs of retinal damage were used to identify the sites of the original RD.

Overall, XIAP-treated detached retinas showed greatly preserved retinal structure in comparison

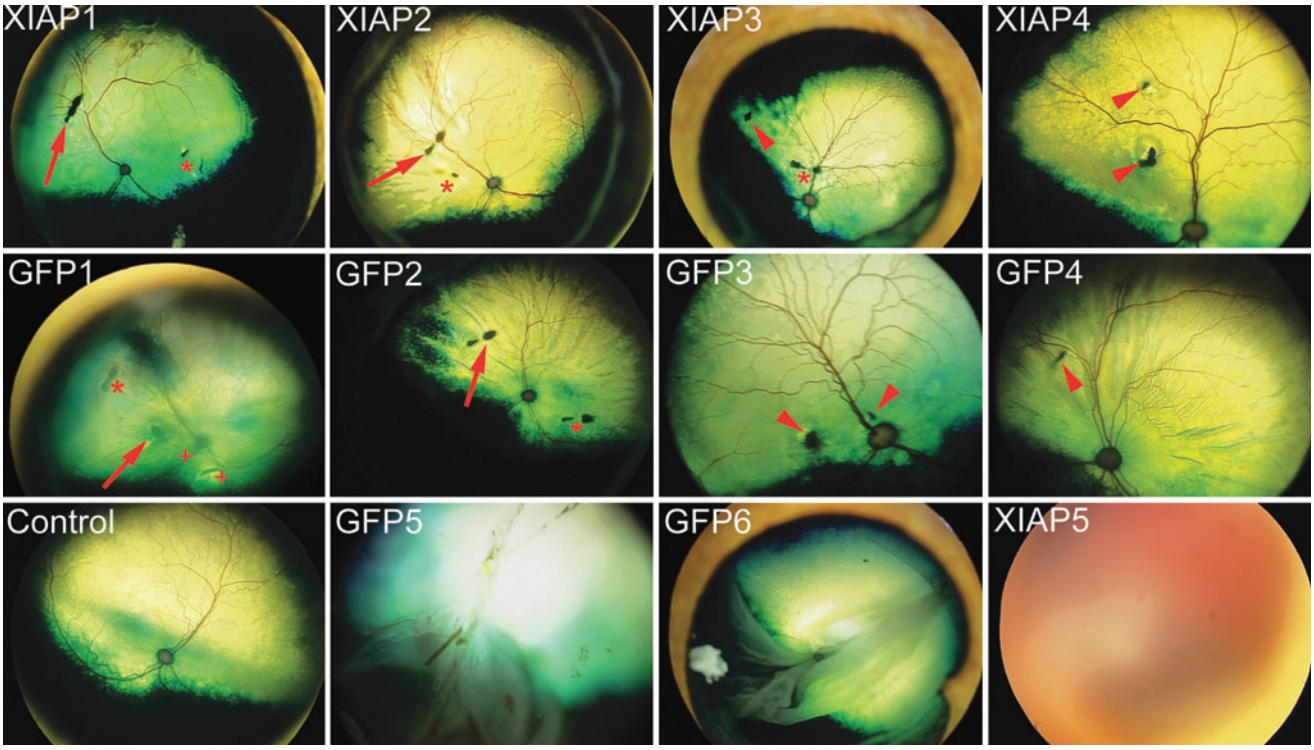

Figure 3. Fundus images of the animals at the endpoint of the experiment. The retinotomies created by the vector injection (*asterisk*) and by the detachment (*arrow*) are visible in most of the fundus images. *Arrowheads* are used to identify retinotomies that could not be specifically assigned to the viral or gas injection based on the video of the surgery or the surgical notes. In GFP1, a solid detachment prevented the acquisition of a clear fundus image, and "+" symbols identify two damaged areas of the retina that cannot be attributed to the virus or gas injection. GFP5 and GFP6 suffered complete detachments, and XIAP5 shows a vitreal hemorrhage, which developed at later stages in the experiment, preventing the acquisition of a fundus image.

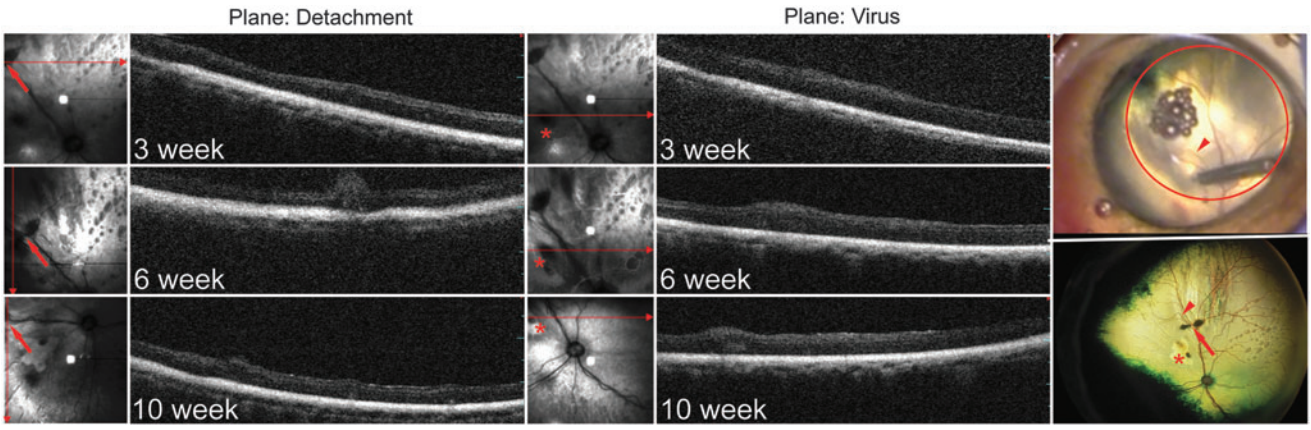

Figure 4. Optical coherence tomography (OCT) images of XIAP-injected, detached retina at various time points after detachment. Panels on the *right* show an image of the cannula making the retinotomy to inject the C_3F_8 gas (*top*) and the fundus image of the retina at 10 weeks after the detachment (*bottom*). The *arrowhead* in both images identifies a minor arching blood vessel, which can be used to identify the retinotomy for the gas injection reproducibly (*arrow*) and for the viral injection (*asterisk*). OCT images on the *left*, through the plane of the gas injection or the virus injection, show that the retina has reattached, with no appearance of abnormal pathology due to the detachment. Small areas of elevation in the OCT may represent large blood vessels.

to GFP-treated detached retinas (Table 1, Fig. 5, and Supplementary Fig. S5). Aside from the XIAP animal with the vitreal and subretinal hemorrhage (which were confirmed by fundus imaging and histology, respectively), three of four XIAP-treated retinas in the nasal plane (and two of four in the plane of the optic nerve) showed a completely intact photoreceptor layer. In these animals, there was no evidence of retinal damage whatsoever. This was not seen in any of the GFP-treated animals, which had some evidence of retinal damage in every animal and in both histological planes.

Since RD leads to photoreceptor cell death, damage should be reflected in a reduction in the area occupied by the ONL. In order to assess further the ability of XIAP to protect photoreceptors, the ONL area and the total retinal area were measured in XIAP- and GFP-treated eyes in the superior retina where the detachments were placed, and the ratio of the ONL area to the total retinal area was calculated. The analysis was conducted in the plane of the optic nerve, from the optic disc to a distance of 8,800 μm toward the peripheral retina. The same analysis was conducted in the inferior intact retina to allow comparisons between intact control retinas and GFP- and XIAP-treated detached retinas. Sample measurements are shown in Supplementary Fig. S6. In order to eliminate any source of bias, the analysis was conducted by a researcher who was masked to the experimental status of the eyes. The ratio of ONL area to total retinal area was significantly greater in the XIAP-treated group (Fig. 6A; $p \leq 0.01$) in comparison with the GFP-treated group, indicating greater preservation of

Table 1. *Experimental notes and outcomes for all animals in the study*

	Structural integrity	*Proximity of retinotomies*[a]	*Notes*	*Exclusion from analysis*
XIAP1	+++	Far apart	Incomplete reattachment (retinal puckering)	
XIAP2	+++	Close		
XIAP3	+++++	Close		
XIAP4	+++++	Close		
XIAP5	++	ND	Vitreal hemorrhage	
XIAP6	Complete RD	ND	ND	Excluded from quantification
GFP1	+	Close	Solid partial detachment	
GFP2	+	Far apart		
GFP3	++	Close		
GFP4	++	Close		
GFP5	Complete RD	ND	ND	Excluded from quantification
GFP6	Complete RD	ND	ND	Excluded from quantification

[a]The retinotomies are the surgical incisions made by the virus injection and the detachment.
ND, not done; RD, retinal detachment.

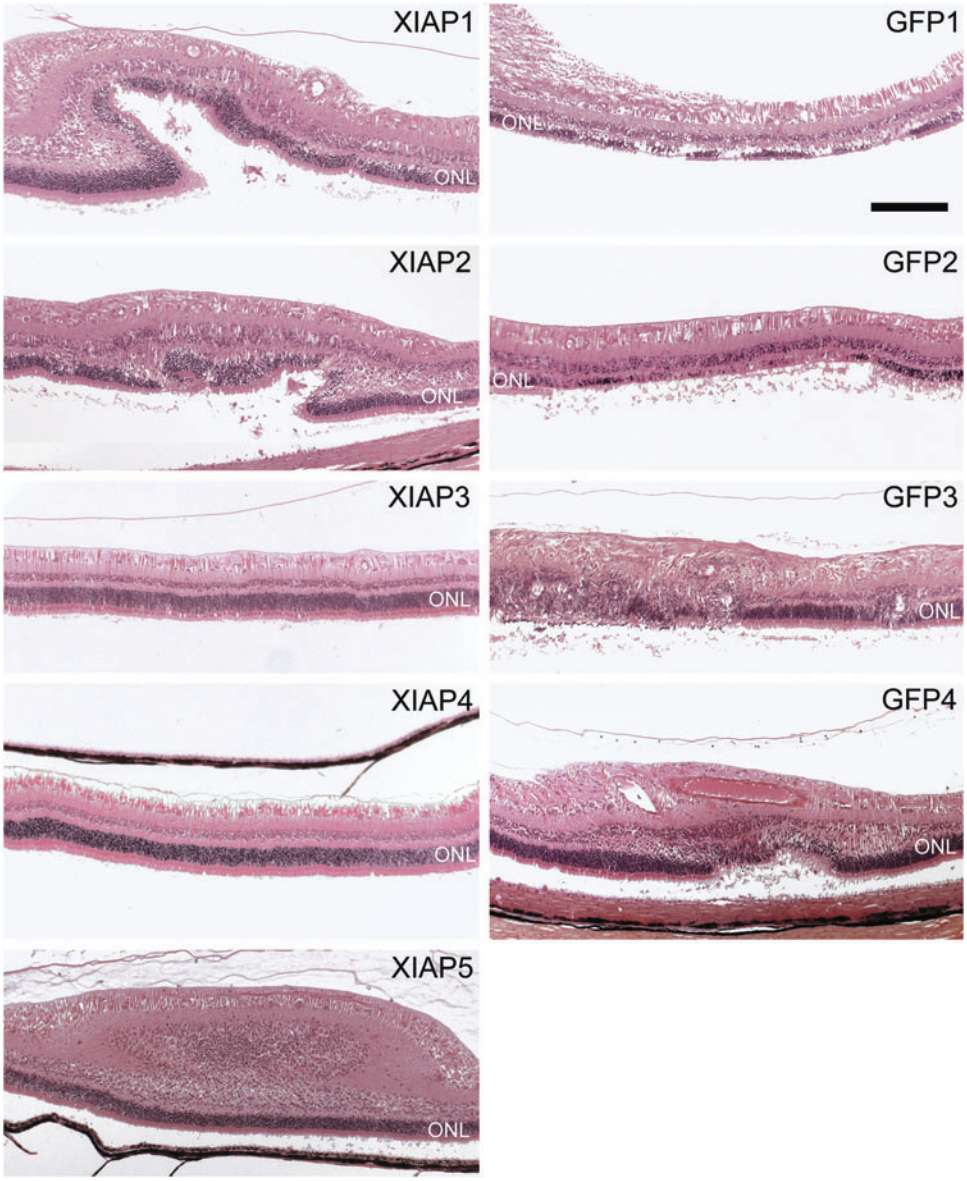

Figure 5. Histological sections in the plane of the optic nerve. Since the retinas had reattached at the time that the eyes were sampled, sections that showed any sign of retinal damage were imaged because it was assumed that the damaged areas were the sites of the retinal detachment. XIAP3 and XIAP4 show perfectly intact retinas with no evidence of damage to the outer nuclear layer (ONL). All green fluorescent protein (GFP) animals show damage resulting from the retinal detachment. GFP1 is the animal with the solid detachment. XIAP5 is the animal with the vitreal hemorrhage. Magnification bar: 100 μm.

photoreceptors following RD. Notably, the XIAP-treated detached retinas and the control intact retinas were not significantly different, suggesting that XIAP was able to preserve ONL integrity. The quantitative analysis of ONL area confirmed the histological observations. In other words, animals that appeared to have the best outcomes according to the histology also showed high ONL/total retina ratios.

Hemagglutinin (HA)-tagged XIAP was localized to the outer and inner segments of the photoreceptor cells near the site of the protected ONL (see Supplementary Fig. S7). Due to autofluorescence of the retinal sections, the GFP protein was more difficult to see, and it necessitated a non-fluorescent colorimetric assay for detection (see Supplementary Fig. S7).

XIAP appears to protect photoreceptor function following RD

Full-field ERGs provide information on retinal function and can be parsed into separate waveforms, each of which is indicative of the health of specific neurons in the retina. The a-wave of the ERG is a measure of photoreceptor health and function. ERGs were taken prior to sampling the

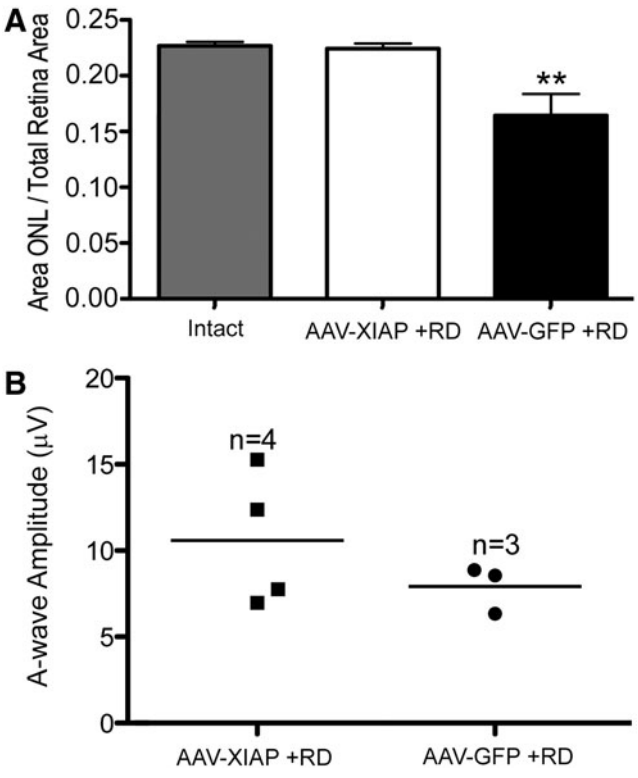

Figure 6. Structural and functional effects on the retina following XIAP therapy. (**A**) XIAP therapy significantly protects photoreceptor structure following retinal detachment in comparison to the GFP-injected detached retina and XIAP-treated detached retina is not significantly different from the intact control. Hematoxylin and eosin images were imported into ImageJ, and were used to calculate the area occupied by the outer nuclear layer (photoreceptors). This was divided by the total retinal area. The analysis was conducted by a researcher who was masked to the experimental status of the animals. Averages represent four GFP animals and five XIAP animals (see Table 1 for animals included in the analysis). The intact inferior retina served as a control. The ONL area of GFP-treated detached retina is significantly reduced in comparison to XIAP-treated retina and to intact control (**$p \leq 0.01$, by one way analysis of variance followed by a Bonferroni *post hoc* analysis). Importantly, XIAP-treated detached retina is not significantly different than intact control retina. Error bars represent SEM. (**B**) Scatter plot showing full-field a-wave ERG amplitudes at the endpoint of the experiment. The values between XIAP-treated and control eyes did not reach significance due to the small number of animals in the analysis ($p = 0.16$, using Student's *t*-test).

eyes in order to assess the ability of XIAP gene therapy to protect photoreceptor function (Fig. 6B). Although there was variability among animals (even in normal intact eyes), the XIAP-treated animals had a-wave amplitudes that were equal to or higher than those of the GFP-treated animals. Importantly, a-wave values appeared to correlate well with histology and ONL area. The highest a-wave value was found in a XIAP-treated animal that also had the best outcomes according to the histology and ONL area, and one of the lowest a-wave values was found in an animal that has surgical complications and imperfect reattachment according to OCT. All animals with full RDs (as well as the solid detachment and retinal hemorrhage animals described above) were removed from the analysis because the surgical complications made the acquisition of a reliable ERG trace difficult. Consequently, the results did not reach significance due to the small numbers of animals remaining ($n = 3$ for GFP and $n = 4$ for XIAP).

DISCUSSION

RD has an incidence of approximately 12/100,000 in the general population, and this translates into a lifetime risk of 0.6% (up to the age of 60 years).[27,28] This risk increases in patients with high myopia.[27] Despite successful surgical interventions to reattach the retina, vision is often compromised in these patients, especially if the central retina (macula) is involved in the detachment.

Animal studies have shown that RD induces both photoreceptor apoptosis and necroptosis. When caspase inhibitors are used to block apoptosis, there is a switch to increased necrotic cell death to compensate for the block in apoptosis.[7] Others have also shown that TNF-α is involved in cell death following RD, further implicating both apoptotic and necrotic pathways.[6] In the current study, overexpression of XIAP protects photoreceptor structure following RD. XIAP is able to protect photoreceptors because in addition to blocking caspases 3, 7, and 9, it has been shown to interact with RIP kinases to reduce the formation of the necroptosome and thus can impact both apoptotic and necroptotic cell death pathways.[16,17,29,30]

In this study, unimpeded activity of the animals resulted in complete detachments in three eyes, necessitating their removal from the study. In addition, further complications with the surgery, including a vitreal and subretinal hemorrhage and the presence of a solid detachment, led to the removal of an additional two animals from the ERG analysis. These complications lowered the power of the study. Nevertheless, significant preservation of the structure of the photoreceptor layer was still found in XIAP-treated detached retinas in comparison with GFP-treated detached retinas. Importantly, XIAP-treated detached retinas were similar in structure to intact controls. In assessing retinal function with ERG, no significant difference was seen between XIAP and GFP. However, higher ERG amplitudes were seen in two of the four XIAP-treated animals, and these two animals also had the best preservation of their photoreceptor layer by histological analysis. There may be several explanations for the imperfect preservation of ONL

function in the other two XIAP-treated animals. In one of these animals (XIAP1; Fig. 3), the fundus image revealed that the retinotomy sites were quite far apart, suggesting that there was imperfect overlap between the viral vector injection and the RD site. Thus, there would have been detached retina that was not covered by the AAV-XIAP injection. Moreover, the presence of puckering in the histological sections (Fig. 5) and the OCTs (see Supplementary Fig. S3) would suggest that the reattachment was not perfect and the photoreceptors might not have received the support that they needed for their continued function. In the clinical setting, this would not be a problem, as retinal reattachment surgery is very successful at ensuring good contact between the retina and the underlying RPE. Therefore, the improved surgical outcomes in the clinic, combined with XIAP therapy, would likely result in robust structural and functional protection of the photoreceptors.

The current study provides proof-of-principle for XIAP efficacy in protecting photoreceptors. However, XIAP gene delivery preceded the RD, in order to allow the virus adequate time to overexpress the transgene prior to the detachment. In the clinical setting, this would not be possible, and the swift onset of retinal damage following a detachment would necessitate rapid intervention to ensure a satisfactory visual outcome. Improved, rapid viral delivery systems would be required. Alternatively, XIAP protein delivery, potentially through the use of biodegradable microparticles,[31,32] would allow immediate delivery of XIAP to the damaged cells and improved outcomes in both retinal structure and function.

ACKNOWLEDGMENTS

We wish to thank Dr. David Zacks (Kellogg Eye Institute) for helping with the detachment protocols, and Renee Torlone and Lijun Fang for help with the surgeries. We are grateful to the Animal Care and Veterinary Service staff for their tremendous help with the surgeries and their wonderful and caring attitude toward the animals in this study. This work was supported by Canadian Institutes of Health Research and Foundation Fighting Blindness Canada grants to C.T. and NIH (grant P30-EY021721), MVRF and RPB, Inc., funding to W.W.H. C.T. is supported by the Don and Joy Maclaren Endowed Chair in Vision Research. S.W. was supported by the David S. Shillito Scholarship in Ophthalmology and by an Ontario Graduate Scholarship.

AUTHOR DISCLOSURE

No competing financial interests exist.

REFERENCES

1. Jalali S. Retinal detachment. Community Eye Health 2003;16:25–26.
2. Erickson PA, Fisher SK, Anderson DH, et al. Retinal detachment in the cat: the outer nuclear and outer plexiform layers. Invest Ophthalmol Vis Sci 1983;24:927–942.
3. Arroyo JG, Yang L, Bula D, et al. Photoreceptor apoptosis in human retinal detachment. Am J Ophthalmol 2005;139:605–610.
4. Huckfeldt RM, Vavvas DG. Neuroprotection for retinal detachment. Int Ophthalmol Clin 2013;53:105–117.
5. Zacks DN, Zheng QD, Han Y, et al. FAS-mediated apoptosis and its relation to intrinsic pathway activation in an experimental model of retinal detachment. Invest Ophthalmol Vis Sci 2004;45:4563–4569.
6. Nakazawa T, Kayama M, Ryu M, et al. Tumor necrosis factor-alpha mediates photoreceptor death in a rodent model of retinal detachment. Invest Ophthalmol Vis Sci 2011;52:1384–1391.
7. Trichonas G, Murakami Y, Thanos A, et al. Receptor interacting protein kinases mediate retinal detachment-induced photoreceptor necrosis and compensate for inhibition of apoptosis. Proc Natl Acad Sci U S A 2010;107:21695–21700.
8. Bertrand MJ, Milutinovic S, Dickson KM, et al. cIAP1 and cIAP2 facilitate cancer cell survival by functioning as E3 ligases that promote RIP1 ubiquitination. Mol Cell 2008;30:689–700.
9. Bertrand MJ, Vandenabeele P. The Ripoptosome: death decision in the cytosol. Mol Cell 2011;43:323–325.
10. Feoktistova M, Geserick P, Kellert B, et al. cIAPs block Ripoptosome formation, a RIP1/caspase-8 containing intracellular cell death complex differentially regulated by cFLIP isoforms. Mol Cell 2011;43:449–463.
11. Leonard KC, Petrin D, Coupland SG, et al. XIAP protection of photoreceptors in animal models of retinitis pigmentosa. PLoS ONE 2007;2:e314.
12. McKinnon SJ, Lehman DM, Tahzib NG, et al. Baculoviral IAP repeat-containing-4 protects optic nerve axons in a rat glaucoma model. Mol Ther 2002;5:780–787.
13. Petrin D, Baker A, Coupland SG, et al. Structural and functional protection of photoreceptors from MNU-induced retinal degeneration by the X-linked inhibitor of apoptosis. Invest Ophthalmol Vis Sci 2003;44:2757–2763.
14. Renwick J, Narang MA, Coupland SG, et al. XIAP-Mediated Neuroprotection in Retinal Ischemia Gene Ther 2006;13:339–347.
15. Zadro-Lamoureux LA, Zacks DN, Baker AN, et al. XIAP effects on retinal detachment-induced photoreceptor apoptosis [corrected]. Invest Ophthalmol Vis Sci 2009;50:1448–1453.
16. Yabal M, Jost PJ. XIAP as a regulator of inflammatory cell death: the TNF and RIP3 angle. Mol Cell Oncol 2015;2:e964622.
17. Yabal M, Muller N, Adler H, et al. XIAP restricts TNF- and RIP3-dependent cell death and in-

flammasome activation. Cell Rep 2014;7:1796–1808.

18. Imre G, Larisch S, Rajalingam K. Ripoptosome: a novel IAP-regulated cell death-signalling platform. J Mol Cell Biol 2011;3:324–326.
19. Wassmer S, Leonard BC, Coupland SG, et al. The Development of a Cat Model of Retinal Detachment and Re-attachment. Adv Exp Med Biol 2016;854:315–321.
20. Hauswirth WW, Lewin AS, Zolotukhin S, et al. Production and purification of recombinant adeno-associated virus. Methods Enzymol 2000;316:743–761.
21. Zolotukhin S, Potter M, Zolotukhin I, et al. Production and purification of serotype 1, 2, and 5 recombinant adeno-associated viral vectors. Methods 2002;28:158–167.
22. Tan E, Ding XQ, Saadi A, et al. Expression of cone-photoreceptor-specific antigens in a cell line derived from retinal tumors in transgenic mice. Invest Ophthalmol Vis Sci 2004;45:764–768.
23. Nayagam DA, McGowan C, Villalobos J, et al. Techniques for processing eyes implanted with a retinal prosthesis for localized histopathological analysis. J Vis Exp 2015;52348.
24. Cederlund M, Ghosh F, Arner K, et al. Vitreous levels of oxidative stress biomarkers and the radical-scavenger alpha1-microglobulin/A1M in human rhegmatogenous retinal detachment. Graefes Arch Clin Exp Ophthalmol 2013;251:725–732.
25. Huang W, Li G, Qiu J, et al. Protective effects of resveratrol in experimental retinal detachment. PLoS One 2013;8:e75735.
26. Roh MI, Murakami Y, Thanos A, et al. Edaravone, an ROS scavenger, ameliorates photoreceptor cell death after experimental retinal detachment. Invest Ophthalmol Vis Sci 2011;52:3825–3831.
27. Haimann MH, Burton TC, Brown CK. Epidemiology of retinal detachment. Arch Ophthalmol 1982;100:289–292.
28. Sodhi A, Leung LS, Do DV, et al. Recent trends in the management of rhegmatogenous retinal detachment. Surv Ophthalmol 2008;53:50–67.
29. Lawlor KE, Khan N, Mildenhall A, et al. RIPK3 promotes cell death and NLRP3 inflammasome activation in the absence of MLKL. Nat Commun 2015;6:6282.
30. Vince JE, Wong WW, Gentle I, et al. Inhibitor of apoptosis proteins limit RIP3 kinase-dependent interleukin-1 activation. Immunity 2012;36:215–227.
31. Rafat M, Cleroux CA, Fong WG, et al. PEG-PLA microparticles for encapsulation and delivery of Tat-EGFP to retinal cells. Biomaterials;31:3414–3421.
32. Wassmer S, Rafat M, Fong WG, et al. Chitosan microparticles for delivery of proteins to the retina. Acta Biomater 2013;9:7855–7864.

Received for publication November 2, 2016;
accepted after revision March 16, 2017.

Published online: March 23, 2017.